



Published in final edited form as:

J Immunol. 2018 September 15; 201(6): 1727–1734. doi:10.4049/jimmunol.1701450.

Glatiramer acetate enhances myeloid-derived suppressor cell function via recognition of paired immunoglobulin-like receptor-B

William van der Touw^{*,**}, Kyeongah Kang^{*,†,**}, Yi Luan^{*}, Ge Ma^{*}, Sunny Mai^{*,†}, Lihui Qin[‡], Guanglin Bian^{*}, Ruihua Zhang^{*}, Sathish Kumar Mungamuri^{*}, Hong-Ming Hu[§], Cheng Cheng Zhang[¶], Stuart A. Aaronson^{*}, Marc Feldmann^{||}, Wen-Chin Yang[#], Shu-Hsia Chen^{*,†}, and Ping-Ying Pan^{*,†}

^{*}Department of Oncological Sciences, Icahn School of Medicine at Mount Sinai, New York, NY, USA

[†]Immunotherapy Research Center, Houston Methodist Research Institute, Houston, TX, USA

[‡]Department of Pathology; Weill Cornell Medical College, New York, NY, USA

[§]Laboratory of Cancer Immunobiology, Earle A. Chiles Research Institute; Providence Portland Medical Center, Portland, OR, USA

[¶]Departments of Physiology and Developmental Biology; University of Texas Southwestern Medical Center, Dallas, TX, USA

^{||}Kennedy Institute of Rheumatology, Nuffield Department of Orthopedics, Rheumatology, and Musculoskeletal science; University of Oxford, Oxford, UK

[#]Agricultural Biotechnology Research Center; Academia Sinica, Taipei, Taiwan

Abstract

Glatiramer acetate (GA, Copaxone) is a copolymer therapeutic FDA approved for the relapsing-remitting form of multiple sclerosis. Despite an unclear mechanism of action, studies have shown that GA promotes protective Th2 immunity and stimulates release of cytokines that suppress autoimmunity. Here we demonstrate that GA interacts with murine paired immunoglobulin-like receptor-B (PIR-B) on myeloid-derived suppressor cells (MDSC) and suppresses the STAT1/NF- κ B pathways while promoting IL-10/TGF β cytokine release. In inflammatory bowel disease models, GA enhanced MDSC-dependent CD4⁺ regulatory T cell (T_{reg}) generation while reducing proinflammatory cytokine secretion. Human monocyte-derived macrophages responded to GA by reducing TNF α production and promoting CD163 expression typical of alternative maturation despite the presence of GM-CSF. Furthermore, GA competitively interacts with leukocyte immunoglobulin like receptors B (LILRBs), the human orthologs of PIR-B. Because GA limited pro-inflammatory activation of myeloid cells, therapeutics that target LILRBs represent novel treatment modalities for autoimmune indications.

Correspondence should be addressed to S.H.C (shuhsia.chen@houstonmethodist.org) and P.Y.P (ppan@houstonmethodist.org). Immunotherapy Research Center, Houston Methodist Research Institute, 6670 Bertner Ave, Houston, TX 77030, USA.

^{**}These authors contributed equally.

Introduction

GA is an FDA approved peptide-based drug for patients with the relapsing-remitting form of multiple-sclerosis and ameliorates models of autoimmunity including autoimmune encephalomyelitis (EAE) (1), colitis (2), and graft-versus-host disease (3, 4). Originally designed to compete for peptide binding to MHC-II (5, 6), GA was hypothesized to act as a decoy antigen to promote anergy or tolerance (7, 8). In several studies, GA showed preferential activation of Th2 lineage, enhanced T_{reg} function, and limited CD8⁺ T cell effector function (9). Later studies showed that GA directly promotes alternative activation of monocytes regardless of T cell myelin recognition (10). Thus, GA-induced type II monocytes were sufficient to ameliorate outcomes in EAE models. Others demonstrated that GA inhibited inflammatory cytokine secretion by monocytes and dendritic cells (11–13), suggesting that GA has therapeutic benefit, in part, by suppressing innate immunity.

Classically activated (M1) macrophages generate a pro-inflammatory response to LPS, IFN γ , and GM-CSF and activate NF- κ B, STAT1, and STAT5, respectively. Conversely, alternatively activated (M2) macrophages are immunoregulatory in response to IL-4, IL-13, and M-CSF and preferentially activate STAT3 and STAT6 (14). In mice, monocytic Ly6C⁺ myeloid-derived suppressor cells (MDSC) display similar plasticity and exhibit M1/M2 dichotomy (15). MDSC play important roles in the regulation of the immune response during infection, malignancy, transplantation, and various immune disorders (16–18). PIR-B is a murine receptor whose expression is restricted to B cells and myeloid cells. PIR-B binds MHC-I as well as angiopoietin-like (ANGPTL) family members (19–21). PIR-B signaling promotes SHP1/2 phosphatase activity resulting in attenuated cell activation, suppressed classical immunity, and as we previously showed, the development and function of MDSC (22). Because GA has been implicated in MHC interactions, we hypothesized that GA may alter signaling downstream of the PIR-B on MDSC.

Materials and Methods

Reagents and mice

GA (Teva Neuroscience), anti-PIR-A/B (6C1, BD Biosciences) and anti-PIR-B (R&D, Santa Cruz). GA-FITC was synthesized by desalting GA using Zeba columns (Pierce) followed by fluorescein isothiocyanate conjugation (Pierce). PHA, anti-Gr-1, anti-CD115, anti-F4/80, anti-CD11b, and isotype-matched antibodies were purchased from eBioscience. MCA26 (23) and LLC cells (ATCC # CBL-1642) were subcutaneously (sc) implanted in female BALB/c and C57BL/6 mice, respectively. Wild-type mice were obtained from the Jackson Laboratory (Bar Harbor, ME). Colonies of HA-TCR transgenic (Tg) mice (24), and PIR-B deficient mice (22) were established from the mice generously provided by Drs. C. A. Bona (Icahn School of Medicine at Mount Sinai, New York, NY) and T. Takai (Tohoku University, Japan). Animals were handled in accordance with the institutional animal guidelines.

Preparation of MDSC

MCA26 tumor-bearing BALB/c mice were used to generate murine MDSC *in vivo* as previously described (23). Briefly, mice with tumor sizes greater than 10 × 10 mm² were

sacrificed and MDSC were enriched from total bone marrow cells by Percoll gradient centrifugation (GE Healthcare) as previously reported (25). Cells banding at 50–60% were labeled with anti-CD115 PE (eBioscience) followed by magnetic bead positive selection using anti-PE microbeads (Miltenyi Biotec). For *in vitro* generation of MDSC, mouse bone marrow cells were cultured with 50 ng/ml GM-CSF and 50 ng/ml IL-6 for 5 days.

Suppression and T_{reg} induction by MDSC

Suppressive activity of MDSC was assessed in a peptide-mediated proliferation assay of TCR transgenic T cells (26). Total splenocytes (1×10^5) from HA-TCR mice were co-cultured with serial dilutions of irradiated MDSC in the presence of HA peptide ($^{110}\text{SFERFEIFPKE}^{120}$, Washington Biotec) at 0.5 $\mu\text{g/ml}$. Proliferation was detected by [^3H]-thymidine incorporation and measured by 1450 Microbeta Trilux liquid scintillation counter (Wallac). T_{reg} induction assays were performed as described previously (22). Total splenocytes (4×10^6) from HA-TCR mice were co-cultured with irradiated MDSC (1×10^6) in the presence of HA peptide and GA (50 $\mu\text{g/ml}$) where indicated. The percentage of T_{reg} was assessed using FACSCantoII or FACS Fortessa (BD Biosciences) multiparameter flow cytometer five days later using fluorochrome-conjugated anti-CD4, anti-CD25, and anti-Foxp3 antibodies (eBioscience). FACS data were analyzed using FlowJo software (Treestar).

Cytokine detection by enzyme-linked immunosorbent assay (ELISA)

Culture supernatants were collected for measurement of mouse or human cytokines (IL-6, IL-10, IL-23, IFN γ , TNF α , TGF β 1, and IL-17A) by Ready-Set-Go ELISA kit (eBioscience) according to manufacturer's recommendations.

Immunoprecipitation and immunoblot

MDSC were stimulated with GA for 2 hr, followed by treatment with vehicle, LPS (100 ng/ml), or IFN γ (20 ng/ml) for an additional 30 min. Total cell lysates were prepared for immunoblotting. p-NF- κ B, p-p38, p-STAT1, p-SHP1, β -actin, Tubulin (Cell Signaling Technology), FITC (Thermo Fisher Scientific) and PIR-B (R&D systems) detection antibodies were used according to manufacturer's recommendations. For immunoprecipitation, total cell lysates from CD115⁺ MDSC were incubated with PBS vehicle control or GA-FITC, followed by anti-FITC antibody detection and protein G bead pulldown according to manufacturer's recommendations (Thermo Fisher Scientific). The precipitates and total lysates were analyzed by immunoblot as previously described (22).

Murine colitis model

Colitis was induced in C57BL/6 mice by feeding plain water or water containing 3.5% dextran sulfate sodium (DSS) (Sigma-Aldrich) for 7 days and the body weight was followed. Colitis groups were injected daily with PBS (0.1 ml), GA (150 $\mu\text{g/mouse}$, subcutaneously), and 2 adoptive transfers of MDSC (5×10^6 cells/mouse) on days 1 and 6 where indicated. All animals were graded daily with observations expressed as a clinical score. The clinical score was determined by blinded independent analysis of mice. Weight loss of 0%, 1–5%, 5–10%, 10–20%, and >20% received a score of 0, 1, 2, 3, and 4 respectively. For stool consistency, normal pellets, soft stool, and liquid stool received scores of 0, 2, and 4, respectively.

Bleeding from the anus described as absent, present, or gross presence received scores of 0, 2, and 4, respectively. The average of the three scores was used to calculate clinical score. On day 12, mice were sacrificed and the entire colons were removed. Colon length was measured and pathology scores were determined from 10% formalin-fixed H&E stained histology sections. Pathology of the large intestine was scored by blinded independent analysis. Grade 0 was assigned when no changes were observed; grade 1 indicated minimal infiltration of the lamina propria and/or mild mucosal hyperplasia; grade 2 indicated mild infiltration of the lamina propria with extension into the submucosa, focal erosions, mild hyperplasia and visible mucin depletion; grade 3 indicated mild to moderate infiltration of the lamina propria and submucosa, transmural ulceration and moderate mucosal hyperplasia and mucin depletion; grade 4 indicated transmural infiltration with ulceration, increased hyperplasia and mucin depletion, and multifocal crypt necrosis; grade 5 indicated transmural infiltration with ulceration, widespread crypt necrosis and loss of intestinal structure and glands.

Human monocyte isolation and culture

PBMC were isolated from healthy human donor blood buffy coats (New York Blood Center) by Lymphoprep gradient centrifugation (StemCell Technologies), according to manufacturer's instructions. Myeloid cells were positively selected from PBMC using anti-human CD33 microbeads (Miltenyi Biotec) then cultured in complete RPMI-1640 medium for 5 days in the presence of GA and 50 ng/mL M-CSF (Peprotech) or 50 ng/mL GM-CSF (Peprotech) where indicated. Five days later, viable cells were analyzed by flow cytometry using anti-CD33, anti-CD14, anti-CD16, anti-CD163, anti-CD206, anti-CD86, and isotype-control matched antibodies (eBioscience). An aliquot of the 5-day culture was restimulated with LPS (Sigma-Aldrich) at 50 ng/mL for 16 hours followed by ELISA analysis of the supernatant.

2B4 reporter cell-based assays

2B4 cells expressing NFAT-GFP and DAP12 transgenes were a gift from Hisashi Arase. Primers containing an in-frame XhoI restriction site flanking the extracellular domain of LILRB1, LILRB2, LILRB3, and LILRB4 genes were used for PCR amplification from cDNA plasmids (GE Dharmacon). LILRB extracellular domain was cloned into pMXs-puro retroviral vector (gift from Hisashi Arase) containing an N-terminal SLAM signal peptide and C-terminal murine PILR transmembrane domain separated by XhoI cloning site. pMXs-puro LILRB1, LILRB2, LILRB3, LILRB4 retroviral constructs were generated by XhoI (New England Biolabs) digestion of PCR fragment and XhoI + calf intestinal phosphatase (New England Biolabs) digestion of pMXs-puro vector. DNA fragments were PCR purified or gel extraction purified (Qiagen) followed by T4 DNA Ligase (New England Biolabs) ligation and transformation into DH5alpha competent cells (Life Technologies) according to manufacturers' recommendations. pMXs-puro LILRB transduced 293 MMLV packaging cell lines were used to generate infectious virus to transduce 2B4 cells over 48 hours. Positive transduced cells were isolated using PE-conjugated anti-LILRB1, anti-LILRB2, anti-LILRB3, and anti-LILRB4 (eBioscience) labeled cells followed by FACS sorting (BD FACSAria). Non-transduced, LILRB1, LILRB2, and LILRB3 transduced 2B4 reporter cells were stimulated with anti-CD3 (eBioscience), anti-LILRB1 (R&D Systems), anti-LILRB2

(BioLegend), or anti-LILRB3 (R&D Systems). LILRB4 antibody (9F4) was internally developed by hybridoma cloning following LILRB4 immunization of mice. Antibodies were coated onto 96-well tissue culture plates and cells were stimulated 16 hours in the presence of GA followed by measurement of GFP by flow cytometry.

Statistical analysis

Statistical analyses were performed using Student's T-test. The results are presented as mean \pm SD. A P value of < 0.05 was considered to be statistically significant.

Results

GA reduces proinflammatory responses on MDSC through binding to PIR-B

Because GA was previously shown to limit TNF α and IL-12 release in innate immune cells, we investigated whether GA suppresses M1-like MDSC maturation. Monocytic MDSC isolated from wild-type tumor-bearing mice were stimulated *ex vivo* in the presence of IFN γ or LPS. 2 hours of GA pretreatment was sufficient to suppress STAT1, p38, and NF- κ B phosphorylation (Fig. 1A). GA suppressed LPS-induced TNF α and IL-6 production while enhancing IL-10 and TGF β regulatory cytokines (Fig. 1B). We previously showed that PIR-B modulates MDSC polarization by inhibiting LPS and IFN γ mediated activation of MAPK, NF- κ B, and STAT1 (22). Because GA variably binds murine MHC-I and MHC-II (6), we hypothesized that GA may alter myeloid cell activation by modulating PIR-B signaling. PIR-B deficiency skews MDSC maturation to an M1 phenotype by enhancing TNF α secretion while lowering IL-10 (22). We observed that *ex vivo* GA-treated wild-type (WT) MDSC produced less TNF α and more IL-10; no significant change in cytokine levels was observed in GA-treated PIR-B^{-/-} MDSC (Fig. 1C) and, GA treatment did not alter expression of co-stimulatory or inhibitory receptors (data not shown). To determine whether GA altered the myeloid cell phenotype by binding PIR-B, we analyzed interactions between GA and PIR-B. FITC-conjugated GA specifically stained WT MDSC, similarly to anti-PIR-B or FLAG-tagged recombinant Angiopoietin-like 2 (ANGPTL2), a natural ligand of PIR-B (21). Unconjugated GA blocked this interaction in WT but not PIR-B^{-/-} MDSC (Fig. 1D). The interaction of GA with PIR-B was further confirmed by co-immunoprecipitation. Anti-FITC magnetic beads bound to FITC-conjugated GA pulled down PIR-B from WT MDSC lysates (Fig. 1E). PIR-B contains multiple cytoplasmic ITIM motifs known to associate with SHP-1 (27). Immunoblotting for phosphorylated SHP-1 (Y564) on anti-PIR-B immunoprecipitated WT MDSC lysates demonstrated acute activation of SHP-1 on PIR-B in response to GA, but not from PIR-B^{-/-} MDSC lysate (Fig. 1F). We concluded that GA binds PIR-B on MDSC to inhibit classical activation of proinflammatory cytokine release.

GA promotes MDSC-induced Treg expansion

Multiple pathways including inhibition of T cell activation and induction of T_{reg} have been proposed to explain how MDSC with M2-like properties suppress adaptive immunity (16). We ascertained whether GA treatment alters an effect of MDSC on T cell maturation and activation. To study antigen-specific T cell responses, we stimulated splenocytes from mice expressing a HA-specific transgenic T cell receptor (TCR) on CD4⁺ T cells with HA peptide in the presence of MDSC. MDSC-mediated suppression of T cell proliferation was

unaffected by the presence of GA (Fig. 2A), but GA further promoted MDSC-dependent CD25⁺Foxp3⁺ T_{reg} conversion (Fig. 2B). We also found that GA had no influence on MDSC-mediated T cell suppression when PIRB KO MDSCs were cocultured with total splenocytes (Fig. S1A). Analyses of cytokine profiles indicated that MDSC and GA both contributed to reduction of IL-17 (Fig. 2C). In the presence of MDSC, GA specifically enhanced IL-10 and TGFβ while reducing IL-23 and IL-6 (Fig. 2D), thus favoring conditions that suppress Th17 maturation but enhance T_{reg} induction. We conclude that the T_{reg}-promoting properties of GA result, in part, from altered cytokine release from innate immune cells. These findings also provide a potential mechanism for how GA ameliorates MS.

GA ameliorates DSS-induced colitis by sustaining M2 functional MDSC

We next assessed the therapeutic efficacy of administering GA in combination with MDSC. Mice given DSS-supplemented water develop acute colitis and GA treatment can ameliorate symptoms (28). Adoptive transfer of MDSC significantly decreased disease onset and GA treatment in combination with MDSC achieved the best efficacy in suppressing the development of IBD (Fig. 3A). Similar observations were made when assessing treatment efficacy based on colon length (Fig. 3B) and pathological scores (Fig. 3C, Fig. S2A). Furthermore, we found that mice treated with MDSC+GA had significantly higher TGFβ and IL-10, and significantly lower IFNγ and IL-17A in the colon when compared to untreated DSS IBD mice (Fig. S2B). Cells isolated from the mesenteric lymph nodes of day 12 DSS IBD mice were analyzed for their reactivity *ex vivo*. Upon restimulation with PHA, T cell proliferation was decreased in mice treated with MDSC and further decreased when combined with GA compared to the control group (Fig. 3D). Mice treated with MDSC had a higher percentage of CD4⁺CD25⁺FoxP3⁺ T_{reg} in mesenteric lymph nodes. This effect was enhanced by treatment with GA (Fig. 3E). The results suggest that GA helps to sustain an M2-functional like MDSC to ameliorate IBD.

In order to confirm whether PIR-B is necessary for the therapeutic efficacy of GA in combination with MDSC, PIR-B KO MDSCs were transferred to mice during DSS administration. Adoptive transfer of PIR-B KO MDSC with GA exhibited no suppressive efficacy on the development of IBD (Fig. 3F and G, Fig. S3). Rather, PIR-B KO MDSC transfer induced slightly more severe IBD development with reducing the body weight and shorter colon length (Fig. 3F and G, Fig. S3). Further, T cell proliferation was not decreased in mice treated with PIR-B KO MDSC whereas WT MDSC treatment significantly decreased T cell proliferation (Fig. 3H). Thus, these results indicate that PIR-B is required for GA to sustain an M2-like phenotype in MDSCs and to ameliorate IBD.

GA controls inflammatory responses in human myeloid cells and binds to human orthologs of PIR-B

To determine if GA exerts a similar mechanism of action in human myeloid cells, we stimulated CD33⁺ human monocytes from healthy donors (n=16) in the presence of LPS and GA. TNFα secretion was suppressed while TGFβ was enhanced (Fig. 4A), suggesting that GA treatment could dampen the monocyte proinflammatory response. However, monocyte-released IL-10 was not significantly enhanced in contrast to murine MDSC. To determine if

GA had more potent activity in suppressing inflammation from M1-skewed human macrophages; monocyte-derived macrophages (MDM) were generated by culturing human monocytes with GM-CSF and GA for 5 days, where indicated. In response to LPS restimulation, GA potently inhibited TNF α secretion in M1-like MDM (Fig. 4B). Levels of detectable IL-10 were unchanged in response to GA (data not shown).

CD163, a scavenger receptor for the hemoglobin-haptoglobin complex, is expressed on subsets of myeloid cells and macrophages. Its expression on the cell surface is correlated with anti-inflammatory responses and is an indicator of poor prognosis in a variety of cancers (29, 30). CD163 surface expression is enhanced in the presence of M-CSF, IL-6, IL-10, and in response to glucocorticoids (31). Meanwhile, inflammatory signals including GM-CSF, LPS, IFN γ , and TNF α inhibit CD163. Despite the presence of GM-CSF in 5-day monocyte-derived-macrophage cultures, GA rescued CD163 expression in some donors at various concentrations (Fig. 4C, Fig. S4A). Expression of CD16 also correlated with CD163 in response to GA. Varying dose-dependent expression of CD163 may be due to donor-specific responsiveness to GA. Based on murine data with PIR-B, we further determined if GA could functionally bind to human orthologs of PIR-B. Unlike mice, humans express five receptors (LILRB1, LILRB2, LILRB3, LILRB4, and LILRB5) that are functionally related to, but distinct from mouse PIR-B. Like PIR-B, LILRB1 and LILRB2 recognize human MHC-I (32) and ANGPTL family members (21) whereas LILRB3 and LILRB4 ligand binding remains poorly defined. To determine if GA interacts with LILRBs, we utilized the 2B4 NFAT-GFP reporter assay originally described in studies of the structurally related NK cell receptors (33) and subsequently adapted to study LILRB receptor activation. Crosslink activation of the LILRB extracellular domain stimulates DAP12-dependent calcium flux leading to NFAT-dependent GFP transcription. We generated LILRB1, LILRB2, LILRB3, and LILRB4 specific NFAT-GFP reporter cell lines to determine if GA could alter receptor crosslink-dependent activation. Plate-bound antibodies to LILRB1, LILRB2, LILRB3, and LILRB4 were able to activate NFAT-GFP in a dose-dependent manner (Fig. S4B). Interestingly, soluble GA competed with LILRB2 and LILRB3 and inhibited antibody-dependent crosslink activation, also in a dose-dependent manner (Fig. 4D–E). LILRB1 and LILRB4 activation was not significantly altered in response to GA as compared to the parental cell line positive control (TCR stimulation). Our data suggest that a peptide component of GA is capable of competing with antibodies for LILRB2 and LILRB3 binding.

Discussion

We have identified that murine PIR-B and human orthologs LILRB2 and LILRB3 are novel targets for GA, an FDA-approved immunotherapeutic that suppresses classical activation of monocytes and promotes M2-like monocytic MDSC populations. LILRB and PIR-B have been well known to regulate maturation and to suppress activation of myeloid cells including MDSC, macrophages, mast cells, neutrophils, dendritic cells, and B cells (34, 35). LILRB and PIR-B are ITIM-containing receptors. ITIM-containing receptors have been known to bind to 3 groups of ligands; membrane-bound proteins, including MHC class I or HLA class I, extracellular matrix proteins, and soluble proteins such as Fc γ RIIB (35). PIR-B and LILRB2 have known ligands including MHC class I, Angptls, β -amyloid, myelin inhibitors,

and CD1d. No ligands have been identified for LILRB3 (35). GA has been known to associate with MHC class II molecules and compete with myelin antigens (9, 36). However, studies indicated that antagonism of MHC class II might not be the primary mechanism of GA (9, 37). We found that GA can be associated with PIR-B and its human orthologs LILRB2 and LILRB3 (Fig. 1E) not only identifying a potential new ligand for PIR-B/LILRB but also a novel mechanism of GA in the immune system.

GA has been shown to reduce inflammatory cytokine production and M1-like maturation. GA reduced CD40, CD86 and IL-12 expression while enhancing expansion of CD14⁺CD16⁺ cells in PBMC from multiple sclerosis patients (38). Further, GA attenuated TNF- α -induced IRF-1 upregulation and NO production through inhibition of STAT1 activation (39). Consistent with the reported immunosuppressive effects on myeloid cell populations, we show that GA attenuates TNF- α and IL-6 release while enhancing TGF β and IL-10 secretion in murine MDSC. GA treatment further correlated with enhanced SHP-1 phosphorylation of PIR-B, a mechanism we previously showed to promote MDSC M2-like maturation (22). GA promoted MDSC-dependent Treg generation and significantly enhanced the therapeutic effect of MDSC in murine colitis models. The *in vivo* tolerogenic effect of GA-treated MDSCs might be due to both functional changes in MDSC, as well as, GA-treated MDSC-mediated Treg induction. MDSCs and Treg are major cells having immunosuppressive function. The immunosuppressive function of MDSCs in IBD is well known. PMN-MDSC are accumulated in murine colitis models as well as in the peripheral blood of IBD patients suggesting their critical roles in IBD (40). However, the roles of MDSCs in IBD models is quite controversial since they can also function as pro-inflammatory myeloid cells. One of the reasons for the contradictory roles of MDSCs is related to IL-17 production (41). Th17 cells have pathogenic effects in intestinal inflammation (41, 42). In our study, we found that MDSCs reduced IL-17 production and GA enhanced MDSCs-mediated reduction of IL-17 production while increasing Treg expansion. Patients with IBD have been found to harbor reduced peripheral Treg cells (43). Treg cells can suppress inflammatory responses by inhibiting Th17 responses through regulation of TGF- β (44,45). Thus, Treg cells are a promising target to treat intestinal inflammation including Crohn's disease and IBD (45). Since current drug therapies are unable to maintain long-term remission, GA will be a good candidate for clinical therapy in intestinal inflammatory diseases. We performed similar studies on human monocytes and MDM cultures and found that GA acutely suppressed TNF- α secretion. Interestingly, the efficacy of CD16 and CD163 upregulation by GA differed between donors, which is not surprising given the varying efficacies seen in MS patients. These human data suggest that GA can promote alternative macrophage activation. We provide further evidence to support the interaction between GA and human LILRB2 and LILRB3. Regulation or activation of the LILRB family of receptors may be responsible for GA-dependent alternative activation in human monocytes and macrophages. We suggest further investigation in this area to explore the use of LILRB-targeted interventions on human myeloid populations to improve upon the immunoregulatory changes observed in macrophage maturation in response to GA.

Supplementary Material

Refer to Web version on PubMed Central for supplementary material.

Acknowledgments

This work was supported in part by grants from the National Cancer Institute to S.-H. Chen (R01CA109322, R01CA127483, R01 CA 208703 and Kaohsiung Medical University Research foundation I05KMUOR05) and to P.-Y. Pan (R01CA140243 and R01 CA188610). The NCI training grants T32CA078207 and F32AI122715 to Dr. William Vander Touw and T32 GM062754 to Sunny Mai. This work was supported by Methodist Research funds to S.H.C. and P.Y.P.

W.v.d.T. performed human PBMC experiments, reporter assay experiments, and analyzed/interpreted results. Y.L. performed immunoblot experiments. W.C.Y., K.K., R.Z., and G.M. performed mouse experiments and analyzed/interpreted results. S.M. performed cytokine ELISAs. L.Q. for pathology diagnosis and scoring. C.C.Z., H.M.H., S.M. and W.C.Y. created reagents. S.H.C. and P.Y.P. planned and designed the overall research. W.v.d.T., S.A., M.F., W.C.Y., S.H.C., and P.Y.P. wrote and edited the manuscript. We thank Drs. B. Coakley, Lloyd Mayer, Sergio Lira, Huabao Xiong and Zhang Yao for their technical assistance and constructive discussion.

References

- Teitelbaum D, Meshorer A, Hirshfeld T, Arnon R, Sela M. 1971; Suppression of experimental allergic encephalomyelitis by a synthetic polypeptide. *Eur J Immunol.* 1:242–248. [PubMed: 5157960]
- Aharoni R, Kayhan B, Arnon R. 2005; Therapeutic effect of the immunomodulator glatiramer acetate on trinitrobenzene sulfonic acid-induced experimental colitis. *Inflammatory bowel diseases.* 11:106–115. [PubMed: 15677903]
- Arnon R, Aharoni R. 2004; Mechanism of action of glatiramer acetate in multiple sclerosis and its potential for the development of new applications. *Proceedings of the National Academy of Sciences of the United States of America.* 101(Suppl 2):14593–14598. [PubMed: 15371592]
- Kerschensteiner M, Stadelmann C, Dechant G, Wekerle H, Hohlfeld R. 2003; Neurotrophic cross-talk between the nervous and immune systems: implications for neurological diseases. *Annals of neurology.* 53:292–304. [PubMed: 12601697]
- Fridkis-Hareli M, Strominger JL. 1998; Promiscuous binding of synthetic copolymer 1 to purified HLA-DR molecules. *Journal of immunology.* 160:4386–4397.
- Fridkis-Hareli M, Teitelbaum D, Gurevich E, Pecht I, Brautbar C, Kwon OJ, Brenner T, Arnon R, Sela M. 1994; Direct binding of myelin basic protein and synthetic copolymer 1 to class II major histocompatibility complex molecules on living antigen-presenting cells--specificity and promiscuity. *Proceedings of the National Academy of Sciences of the United States of America.* 91:4872–4876. [PubMed: 7515181]
- Neuhaus O, Farina C, Yassouridis A, Wiendl H, Then Bergh F, Dose T, Wekerle H, Hohlfeld R. 2000; Multiple sclerosis: comparison of copolymer-1- reactive T cell lines from treated and untreated subjects reveals cytokine shift from T helper 1 to T helper 2 cells. *Proceedings of the National Academy of Sciences of the United States of America.* 97:7452–7457. [PubMed: 10861011]
- Teitelbaum D, Milo R, Arnon R, Sela M. 1992; Synthetic copolymer 1 inhibits human T-cell lines specific for myelin basic protein. *Proceedings of the National Academy of Sciences of the United States of America.* 89:137–141. [PubMed: 1370347]
- Laliv PH, Neuhaus O, Benkhoucha M, Burger D, Hohlfeld R, Zamvil SS, Weber MS. 2011; Glatiramer acetate in the treatment of multiple sclerosis: emerging concepts regarding its mechanism of action. *CNS Drugs.* 25:401–414. [PubMed: 21476611]
- Weber MS, Prod'homme T, Youssef S, Dunn SE, Rundle CD, Lee L, Patarroyo JC, Stuve O, Sobel RA, Steinman L, Zamvil SS. 2007; Type II monocytes modulate T cell-mediated central nervous system autoimmune disease. *Nature medicine.* 13:935–943.
- Vieira PL, Heystek HC, Wormmeester J, Wierenga EA, Kapsenberg ML. 2003; Glatiramer acetate (copolymer-1, copaxone) promotes Th2 cell development and increased IL-10 production through modulation of dendritic cells. *Journal of immunology.* 170:4483–4488.
- Weber MS, Starck M, Wagenpfeil S, Meinl E, Hohlfeld R, Farina C. 2004; Multiple sclerosis: glatiramer acetate inhibits monocyte reactivity in vitro and in vivo. *Brain : a journal of neurology.* 127:1370–1378. [PubMed: 15090474]

13. Kim HJ, Ifergan I, Antel JP, Seguin R, Duddy M, Lapierre Y, Jalili F, Bar-Or A. 2004; Type 2 monocyte and microglia differentiation mediated by glatiramer acetate therapy in patients with multiple sclerosis. *Journal of immunology*. 172:7144–7153.
14. Sica A, Mantovani A. 2012; Macrophage plasticity and polarization: in vivo veritas. *J Clin Invest*. 122:787–795. [PubMed: 22378047]
15. Umemura N, Saio M, Suwa T, Kitoh Y, Bai J, Nonaka K, Ouyang GF, Okada M, Balazs M, Adany R, Shibata T, Takami T. 2008; Tumor-infiltrating myeloid-derived suppressor cells are pleiotropic-inflamed monocytes/macrophages that bear M1- and M2-type characteristics. *Journal of leukocyte biology*. 83:1136–1144. [PubMed: 18285406]
16. Gabrilovich DI, Nagaraj S. 2009; Myeloid-derived suppressor cells as regulators of the immune system. *Nat Rev Immunol*. 9:162–174. [PubMed: 19197294]
17. Yin B, Ma G, Yen CY, Zhou Z, Wang GX, Divino CM, Casares S, Chen SH, Yang WC, Pan PY. 2010; Myeloid-derived suppressor cells prevent type 1 diabetes in murine models. *Journal of immunology*. 185:5828–5834.
18. Garcia MR, Ledgerwood L, Yang Y, Xu J, Lal G, Burrell B, Ma G, Hashimoto D, Li Y, Boros P, Grisotto M, van Rooijen N, Matesanz R, Tacke F, Ginhoux F, Ding Y, Chen SH, Randolph G, Merad M, Bromberg JS, Ochando JC. 2010; Monocytic suppressive cells mediate cardiovascular transplantation tolerance in mice. *J Clin Invest*. 120:2486–2496. [PubMed: 20551515]
19. Takai T, Ono M. 2001; Activating and inhibitory nature of the murine paired immunoglobulin-like receptor family. *Immunol Rev*. 181:215–222. [PubMed: 11513143]
20. Masuda A, Nakamura A, Maeda T, Sakamoto Y, Takai T. 2007; Cis binding between inhibitory receptors and MHC class I can regulate mast cell activation. *The Journal of experimental medicine*. 204:907–920. [PubMed: 17420263]
21. Zheng J, Umikawa M, Cui C, Li J, Chen X, Zhang C, Huynh H, Kang X, Silvany R, Wan X, Ye J, Canto AP, Chen SH, Wang HY, Ward ES, Zhang CC. 2012; Inhibitory receptors bind ANGPTLs and support blood stem cells and leukaemia development. *Nature*. 485:656–660. [PubMed: 22660330]
22. Ma G, Pan PY, Eisenstein S, Divino CM, Lowell CA, Takai T, Chen SH. 2011; Paired immunoglobulin-like receptor-B regulates the suppressive function and fate of myeloid-derived suppressor cells. *Immunity*. 34:385–395. [PubMed: 21376641]
23. Huang B, Pan PY, Li Q, Sato AI, Levy DE, Bromberg J, Divino CM, Chen SH. 2006; Gr-1+CD115+ immature myeloid suppressor cells mediate the development of tumor-induced T regulatory cells and T-cell anergy in tumor-bearing host. *Cancer research*. 66:1123–1131. [PubMed: 16424049]
24. Bot A, Casares S, Bot S, von Boehmer H, Bona C. 1998; Cellular mechanisms involved in protection against influenza virus infection in transgenic mice expressing a TCR receptor specific for class II hemagglutinin peptide in CD4+ and CD8+ T cells. *Journal of immunology*. 160:4500–4507.
25. Kusmartsev SA, Li Y, Chen SH. 2000; Gr-1+ myeloid cells derived from tumor-bearing mice inhibit primary T cell activation induced through CD3/CD28 costimulation. *Journal of immunology*. 165:779–785.
26. Pan PY, Wang GX, Yin B, Ozao J, Ku T, Divino CM, Chen SH. 2008; Reversion of immune tolerance in advanced malignancy: modulation of myeloid-derived suppressor cell development by blockade of stem-cell factor function. *Blood*. 111:219–228. [PubMed: 17885078]
27. Blery M, Kubagawa H, Chen CC, Vely F, Cooper MD, Vivier E. 1998; The paired Ig-like receptor PIR-B is an inhibitory receptor that recruits the protein-tyrosine phosphatase SHP-1. *Proceedings of the National Academy of Sciences of the United States of America*. 95:2446–2451. [PubMed: 9482905]
28. Aharoni R, Sonogo H, Brenner O, Eilam R, Arnon R. 2007; The therapeutic effect of glatiramer acetate in a murine model of inflammatory bowel disease is mediated by anti-inflammatory T-cells. *Immunol Lett*. 112:110–119. [PubMed: 17719654]
29. Zaki MA, Wada N, Ikeda J, Shibayama H, Hashimoto K, Yamagami T, Tatsumi Y, Tsukaguchi M, Take H, Tsudo M, Morii E, Aozasa K. 2011; Prognostic implication of types of tumor-associated

- macrophages in Hodgkin lymphoma. *Virchows Archiv : an international journal of pathology*. 459:361–366. [PubMed: 21874508]
30. Ino Y, Yamazaki-Itoh R, Shimada K, Iwasaki M, Kosuge T, Kanai Y, Hiraoka N. 2013; Immune cell infiltration as an indicator of the immune microenvironment of pancreatic cancer. *British journal of cancer*. 108:914–923. [PubMed: 23385730]
 31. Etzerodt A, Moestrup SK. 2013; CD163 and inflammation: biological, diagnostic, and therapeutic aspects. *Antioxidants & redox signaling*. 18:2352–2363. [PubMed: 22900885]
 32. Jones DC, Kosmoliaptis V, Apps R, Lapaque N, Smith I, Kono A, Chang C, Boyle LH, Taylor CJ, Trowsdale J, Allen RL. 2011; HLA class I allelic sequence and conformation regulate leukocyte Ig-like receptor binding. *Journal of immunology*. 186:2990–2997.
 33. Arase H, Mocarski ES, Campbell AE, Hill AB, Lanier LL. 2002; Direct recognition of cytomegalovirus by activating and inhibitory NK cell receptors. *Science*. 296:1323–1326. [PubMed: 11950999]
 34. van der Touw W, Chen HM, Pan PY, Chen SH. 2017; LILRB receptor-mediated regulation of myeloid cell maturation and function. *Cancer Immunol Immunother*. 66:1079–1087. [PubMed: 28638976]
 35. Kang X, Kim J, Deng M, John S, Chen H, Wu G, Phan H, Zhang CC. 2016; Inhibitory leukocyte immunoglobulin-like receptors: Immune checkpoint proteins and tumor sustaining factors. *Cell Cycle*. 15:25–40. [PubMed: 26636629]
 36. Arnon R, Sela M. 2003; Immunomodulation by the copolymer glatiramer acetate. *J Mol Recognit*. 16:412–421. [PubMed: 14732933]
 37. Aharoni R, Schlegel PG, Teitelbaum D, Roikhel-Karpov O, Chen Y, Arnon R, Sela M, Chao NJ. 1997; Studies on the mechanism and specificity of the effect of the synthetic random copolymer GLAT on graft-versus-host disease. *Immunol Lett*. 58:79–87. [PubMed: 9271317]
 38. Chuluundorj D, Harding SA, Abernethy D, La Flamme AC. 2017; Glatiramer acetate treatment normalized the monocyte activation profile in MS patients to that of healthy controls. *Immunol Cell Biol*. 95:297–305. [PubMed: 27694998]
 39. Lu H, Zeng C, Zhao H, Lian L, Dai Y. 2014; Glatiramer acetate inhibits degradation of collagen II by suppressing the activity of interferon regulatory factor-1. *Biochem Biophys Res Commun*. 448:323–328. [PubMed: 24657155]
 40. Haile LA, von Wasielewski R, Gamrekelashvili J, Kruger C, Bachmann O, Westendorf AM, Buer J, Liblau R, Manns MP, Korangy F, Greten TF. 2008; Myeloid-derived suppressor cells in inflammatory bowel disease: a new immunoregulatory pathway. *Gastroenterology*. 135:871–881. 881e871–875. [PubMed: 18674538]
 41. Kim YJ, Chang SY, Ko HJ. 2015; Myeloid-derived suppressor cells in inflammatory bowel disease. *Intest Res*. 13:105–111. [PubMed: 25931994]
 42. Ostanin DV, Bhattacharya D. 2013; Myeloid-derived suppressor cells in the inflammatory bowel diseases. *Inflamm Bowel Dis*. 19:2468–2477. [PubMed: 23811636]
 43. Eastaff-Leung N, Mabarrack N, Barbour A, Cummins A, Barry S. 2010; Foxp3+ regulatory T cells, Th17 effector cells, and cytokine environment in inflammatory bowel disease. *J Clin Immunol*. 30:80–89. [PubMed: 19936899]
 44. Ueno A, Jijon H, Chan R, Ford K, Hirota C, Kaplan GG, Beck PL, Iacucci M, Fort Gasia M, Barkema HW, Panaccione R, Ghosh S. 2013; Increased prevalence of circulating novel IL-17 secreting Foxp3 expressing CD4+ T cells and defective suppressive function of circulating Foxp3+ regulatory cells support plasticity between Th17 and regulatory T cells in inflammatory bowel disease patients. *Inflamm Bowel Dis*. 19:2522–2534. [PubMed: 24097227]
 45. Yamada A, Arakaki R, Saito M, Tsunematsu T, Kudo Y, Ishimaru N. 2016; Role of regulatory T cell in the pathogenesis of inflammatory bowel disease. *World J Gastroenterol*. 22:2195–2205. [PubMed: 26900284]

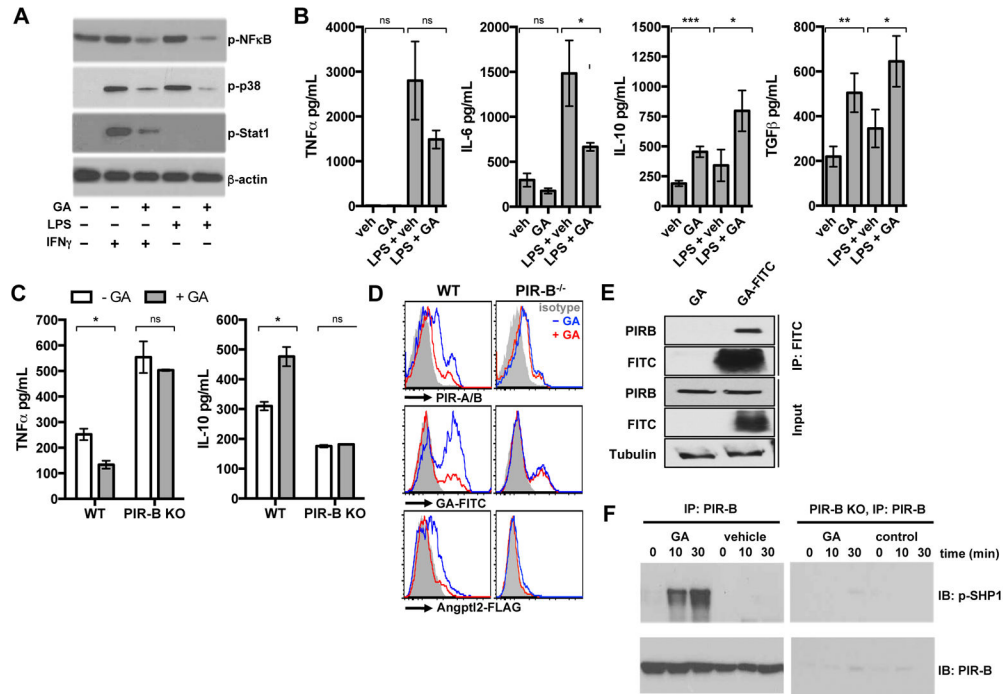


Figure 1. GA restricts classical activation in MDSC via interaction with PIR-B
(A) WT MDSC treated with GA (5 μ g/ml) for 2 hours were stimulated with LPS (100 ng/mL) or IFN γ (20 ng/mL) for 30 min. Immunoblot of lysates detected the phosphorylation of NF- κ B, p38 and STAT1. **(B)** WT MDSC were incubated with GA in the absence or presence of LPS (100 ng/mL) for 30 hours. Secreted TNF α , IL-6, IL-10, and TGF β were quantified by ELISA. **(C)** CD115 $^{+}$ MDSC from LLC tumor-bearing wild-type (WT) or PIR-B $^{-/-}$ hosts were incubated in the absence (white bars) or presence of GA (gray bars) for 24 hours. Secreted TNF α and IL-10 were measured by ELISA. Data (b-c) represent mean \pm s.d. (*, $p < 0.05$; **, $p < 0.005$; ***, $p < 0.0005$; calculated by student's t-test) **(D)** MDSC isolated from WT or PIR-B KO hosts were pre-incubated in the absence (blue line) or presence of GA (red line), washed with cold PBS, and stained for surface PIR-B, GA-FITC, or ANGPTL2-FLAG. FACS data are gated on FSC-A, SSC-A, FSC-W, and DAPI- cells. Histogram data are overlaid FACS staining controls (gray filled). **(E)** Lysates from WT splenocytes incubated with GA or GA-FITC were immunoprecipitated using anti-FITC antibody capture. Precipitates were separated by SDS-PAGE followed by western blot using indicated antibodies. **(F)** WT and PIR-B KO MDSC were treated with GA at time 0, 10, and 30 minutes followed by anti-PIR-B immunoprecipitation. Precipitate was separated by SDS-PAGE followed by probing for phosphorylated SHP-1 and anti-PIR-B.

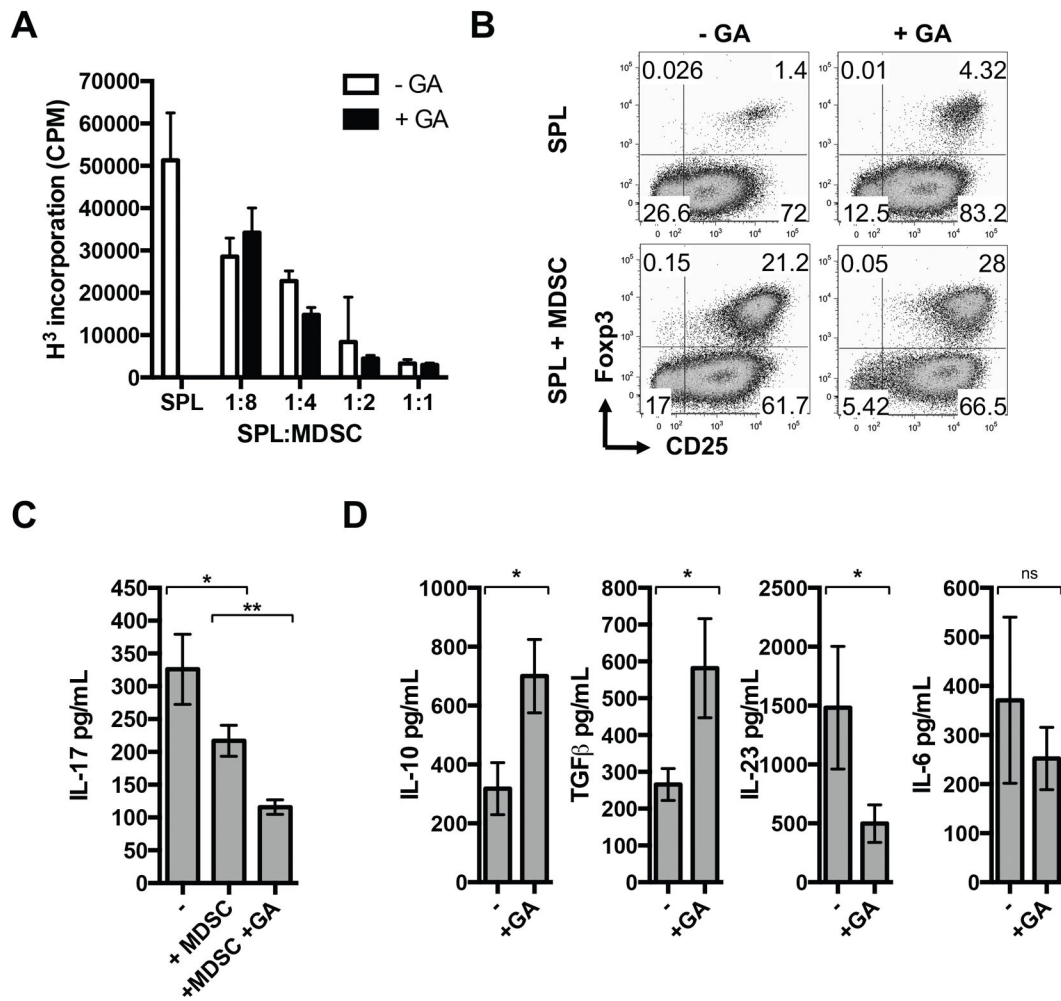


Figure 2. GA enhances MDSC-mediated T_{reg} induction

(A) Splenocytes from CD4 HA-TCR Tg mice (SPL) were co-cultured with HA peptide and indicated ratios of MDSC purified from MCA26-bearing BALB/c mice in the absence (white bars) or presence of GA (5 μg/ml) (black bars). T cell proliferation was assessed by [³H]-Thymidine incorporation. (B) SPL were cultured with HA peptide. Where indicated, MDSC were co-cultured at a ratio of 4:1 in the presence or absence of GA. Splenocyte (SPL) cultures were stained for CD4⁺CD25⁺Foxp3⁺ T_{reg} cells after five days. FACS data are gated on FSC-A, SSC-A, FSC-W, DAPI-, CD3⁺CD4⁺ cells. (C) Secreted IL-17A from cultures in (B) was determined by ELISA. (D) Purified MDSC were stimulated with GA for 24 hours. Secreted IL-10, TGFβ, IL-6, and IL-23 were quantified by ELISA. Data (C–D) represent mean ± s.d. (*, p<0.05; **, p<0.01; calculated by student's t-test)

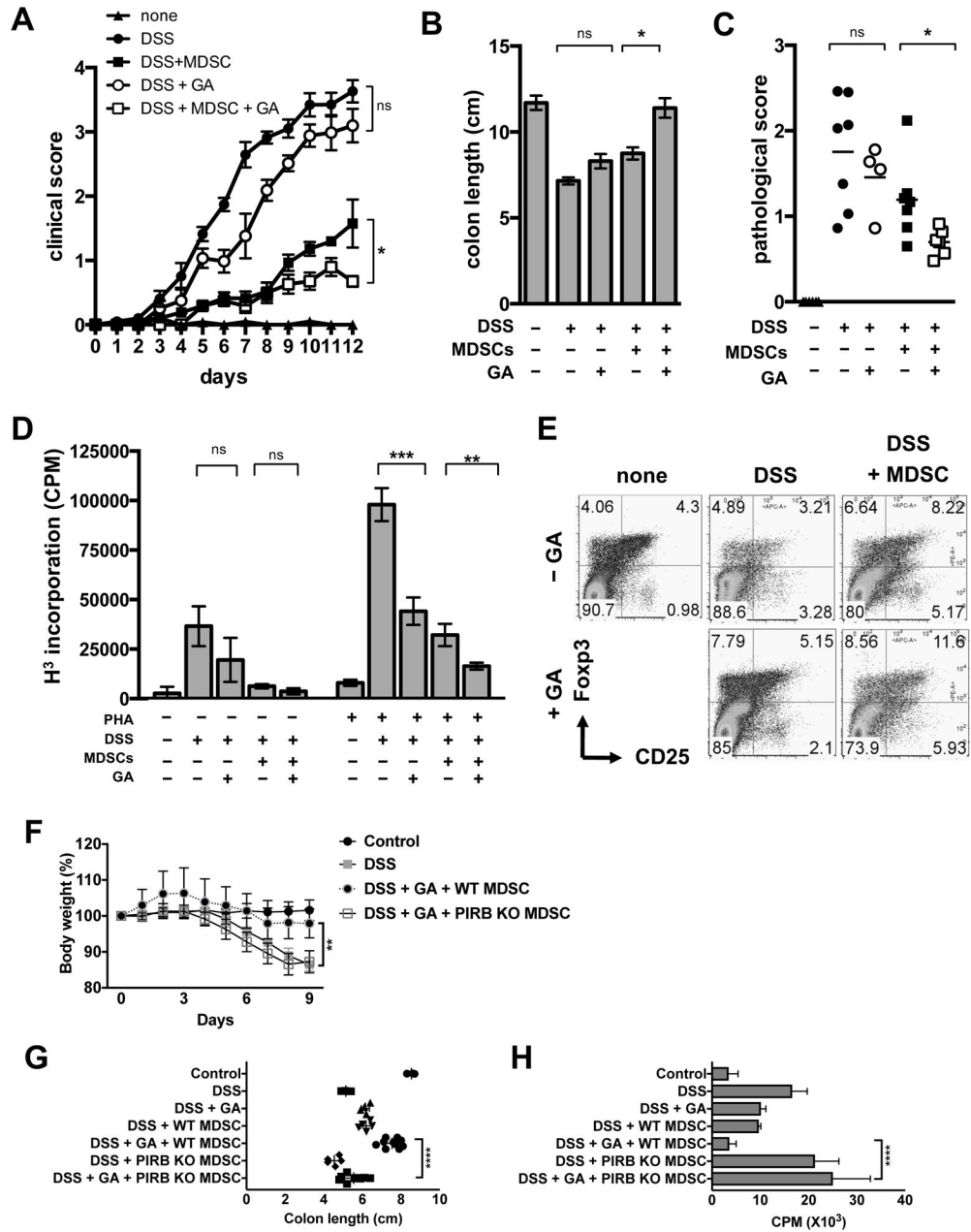


Figure 3. GA enhances MDSC-dependent suppression of DSS-induced colitis
(A) C57BL/6 mice were fed with water containing 3% DSS from day 0 to day 7 to induce colitis. Mice receiving GA were administered a daily injection from day 1 to day 12. Mice receiving MDSC were given intravenous adoptive transfer of MDSC on days 1 and 6. Clinical scores determining the severity of colitis were determined based on stool consistency, rectal bleeding, and weight loss. The data represent the mean changes in clinical scores for each group (5–8 mice per group) from 3 separate experiments. **(B)** Mice from **(A)** were sacrificed on day 12 and colon length measured. **(C)** Colons from **(b)** were fixed and prepared for H&E staining. Inflammation and tissue infiltration were graded blindly for pathological score. **(D)** MLN cells from the mice in **(A)** were isolated and re-stimulated with

vehicle or PHA. [³H]-Thymidine incorporation was used to measure T cell proliferation. (E) MLN cells from the mice in (A) were stained for CD4, CD25, and Foxp3 to detect T_{reg}. FACS data are gated on FSC-A, SSC-A, FSC-W, DAPI-, CD3⁺CD4⁺ cells. Representative dot plots of the MLN cells are shown. (F) C57BL/6 mice were fed water containing 2% DSS from day 0 to day 7 to induce colitis. Mice receiving GA were administered daily injections on days 1 to 9. Mice receiving MDSC were given intravenous adoptive transfer of WT or PIRB KO MDSC on days 1 and 4. Body weight was determined every day. (G) Mice from (F) were sacrificed on day 9 and colon length was measured. (H) MLN cells from the mice in (A) were isolated and cultured for 3 days. [³H]-Thymidine incorporation was used to measure T cell proliferation. Data represent mean ± s.d. (*, p<0.05; **, p<0.01; ***, p<0.001, ****, p<0.0001, calculated by student's t-test)

Author Manuscript

Author Manuscript

Author Manuscript

Author Manuscript

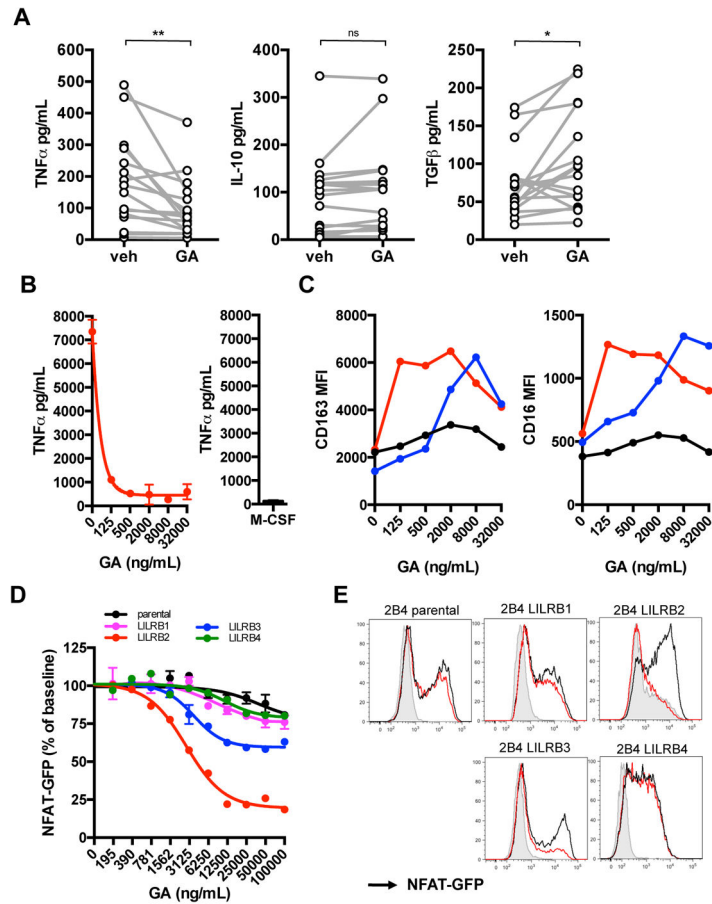


Figure 4. GA inhibits monocyte classical activation via LILRB2/B3 receptor interaction
(A) Human monocytes from healthy donors (n = 16) were stimulated with LPS in the presence of vehicle or GA for 16 hours. Secreted TNF α was measured by ELISA. Data represent paired data for individual donors. (*, p<0.05; **, p<0.005; calculated by paired t-test). **(B)** Human monocytes were matured in the presence of GM-CSF with titrated GA for 5 days. Macrophages were stimulated with LPS for 16 hours and supernatant analyzed for TNF α release by ELISA. M-CSF matured macrophages from the same donor stimulated with LPS are shown as a control. **(C)** Expression of CD163 and CD16 from 5-day human monocyte-derived macrophage maturation in the presence of GM-CSF with titrated GA. Each line represents a different donor. **(D)** 2B4 NFAT-GFP reporter cells stable transduced with LILRB1, LILRB2, LILRB3, or LILRB4 were crosslink activated using LILRB-specific plate-bound antibodies at the EC₅₀ for NFAT-GFP activation. Cells were stimulated in the presence of GA for 16 hours followed by flow cytometry to assess reporter GFP intensity. **(E)** NFAT-GFP MFI expression from 2B4 reporter cells from (D) are unstimulated (gray filled), stimulated in the presence of vehicle control (black line) or 100 μ g/mL GA (red line). FACS data are gated on FSC-A, SSC-A, FSC-W, DAPI- cells.